J Nanopart Res (2013) 15:1777
DOI 10.1007/s11051-013-1777-0

RESEARCH PAPER

Carbon-dot organic surface modifier analysis by solution-state NMR spectroscopy

Aggelos Philippidis · Apostolos Spyros · Demetrios Anglos · Athanasios B. Bourlinos · Radek Zbořil · Emmanuel P. Giannelis

Received: 5 March 2013 / Accepted: 2 June 2013 / Published online: 18 June 2013

Abstract Carbon dots (C-dots) represent a new class of carbon-based materials that were discovered recently and have drawn the interest of the scientific community, particularly because of their attractive optical properties and their potential as fluorescent sensors. Investigation of the chemical structure of C-dots is extremely important for correlating the surface modifier composition with C-dot optical properties and allow for structure–properties fine tuning. In this article, we report the structural analysis of the surface modifiers of three different types of C-dot nanoparticles (Cwax, Cws, and Csalt) by use of 1D- and 2D-high-resolution NMR spectroscopy in solution. We unambiguously verify that the structure of the modifier chains remains chemically unchanged during the passivation procedure, and confirm the covalent attachment of the modifiers to the nanoparticle core, which contributes no signal to the solution-state NMR spectra. To our knowledge, this is the first study confirming the full structural assignment of C-dot organic surface modifiers by use of solution NMR spectroscopy.

Keywords NMR spectroscopy · Carbon dots · Structure · Surface modifiers

A. Philippidis · A. Spyros (✉) · D. Anglos
NMR Laboratory, Department of Chemistry, University of Crete, P.O. Box 2208, Voutes, 710 03 Heraklion, Crete, Greece
e-mail: aspyros@chemistry.uoc.gr

A. Philippidis · D. Anglos
Institute of Electronic Structure and Laser, Foundation for Research and Technology-Hellas (IESL-FORTH), P.O. Box 1385, 711 10 Heraklion, Crete, Greece

A. B. Bourlinos
Physics Department, University of Ioannina, 451 10 Ioannina, Greece

A. B. Bourlinos · R. Zbořil
Regional Centre of Advanced Technologies and Materials, Department of Physical Chemistry, Faculty of Science, Palacky University in Olomouc, 771 46 Olomouc, Czech Republic

E. P. Giannelis
Department of Materials Science and Engineering, Cornell University, Ithaca, NY 14853, USA

Introduction

Recently, a new class of carbon-based nanoparticles that exhibit bright fluorescence has triggered a number of studies for exploring the attractive optical properties of these materials and in particular their potential to act as fluorescence sensors and/or bio-imaging agents (Sun et al. 2006; Cao et al. 2007). Reminiscent, in some respects, of metal or semiconductor quantum dots, also used in fluorescence imaging and sensing applications, these carbon nanoparticles are often termed as carbon dots (abbreviated as C-dots), (Baker and Baker 2010). They are approximately spherical in

shape, with their diameter in the range of 5–10 nm, and consist of a carbon-based core bearing on its surface short or long flexible organic chains. C-dots have been synthesized by various procedures, including, for example, schemes based on laser ablation of graphite, followed by surface functionalization (Sun et al. 2006; Suda et al. 2002), or pyrolytic carbonization of simple precursors that have been found capable to yield functionalized fluorescent nano-particles in a single step (Bourlinos et al. 2008a). While the details of the carbon core structure are not fully illuminated, it is quite clear that the peripheral chains serve two main purposes. They impart high solubility to the C-dots, which can be tailored on the basis of the hydrophobic or hydrophilic character of the chain, but most importantly they are key factors in uncovering the bright fluorescence, built in the C-dots, acting, most likely, as passivating agents for surface energy traps.

In recent reports, we have presented a method for preparing brightly fluorescent C-dots through a pyrolytic route that uses as starting material citrate salts with various amines (Bourlinos et al. 2008a, b). The attractive feature of this route is that the citrate salt anion appears to be preferentially installed, through an amide linkage, as a side chain on the C-dot, enabling diverse solubility properties. By choosing octadecyl amine as a counter ion, a highly non-polar, wax-like, peripheral chain is formed and the resulting C-dot (Cwax) is soluble in non-polar or mildly polar solvents but completely insoluble in polar ones (Bourlinos et al. 2008a). The carbonization of the 2-(2-aminoethoxy)-ethanol counter ion results in water soluble nanoparticles (Cws) (Bourlinos et al. 2008a), while pyrolysis of the ammonium citrate salt formed by use of sodium 18-amino-octadecanoate $[H_2N\text{-}(CH_2)_{18}COO^-Na^+]$ leads to the formation of C-dots with a salt surface functionality (Csalt), which are fully soluble in water and other polar solvents (Bourlinos et al. 2008b).

Transmission electron microscopy (TEM) studies have clearly shown that the three types of C-dot materials investigated consist of nanoparticles (Bourlinos et al. 2008a, b). More specifically, Cwax exhibits a nearly monodisperse size distribution of spherical nanoparticles with an average diameter of 7 nm. Cws and Csalt consist of nearly spherical nanoparticles displaying a broader size distribution with average diameters of 7 and 10–20 nm, respectively. Moreover, the XRD pattern of Cwax displays two superimposed reflections attributed to highly disorder carbon (core) and densely packed alkyl chains (corona), while Cws and Csalt show weaker reflections, indicating a higher amorphous character. The IR absorption spectra of all three C-dots showed bands compatible with the presence of aliphatic chains and amide linkages. No meaningful information was collected via Raman microscopy because of the highly fluorescent nature of the nanoparticles.

The full elucidation of the chemical structure of C-dots is extremely important in order to understand how chemical composition affects optical properties and thus enable their fine tuning. Analytical NMR spectroscopic studies of C-dots can be used to identify the precise structure of the surface modifiers, and establish whether they suffer any chemical alterations during carbonization, to examine the nature of their bonding onto the particle surface and correlate their diffusion dynamics (mobility) to the particle solubility in different solvents. Recently, high-resolution magic angle spinning (HR-MAS) NMR spectroscopy in the solid state has been proposed as an efficient tool for the characterization of organic molecules bound on nanoparticles (Du et al. 2009; Zhou et al. 2008), although CP/MAS and high-resolution solution NMR have also found increased application (Zhang and Yan 2010).

^{31}P CP/MAS and high-resolution NMR spectroscopy has been used to determine the surface structure and size effects on passivated InP quantum dots (Tomaselli et al. 1999), and phosphonic acid capped SnO_2 nanoparticles (Holland et al. 2007). ^{1}H NMR spectroscopy in solution has been used to study the conformation of ethylhexanoate stabilizer adsorbed on to CdS nanoparticles (Diaz et al. 1999), and provided evidence for chemical alterations of oleic acid used as a surfactant during nanocrystal (γ-Fe_2O_3) synthesis (Willis et al. 2005). A study of single-walled ^{13}C-enriched carbon nanotubes (SWNTs) functionalized with diamine-terminated oligomeric poly(ethylene glycol) by ^{13}C NMR spectroscopy in solution has also been reported (Kitaygorodskiy et al. 2005). The ^{13}C NMR spectra of C-dots synthesized from carbon soot and containing an oligomeric PEG diamino surface passive agent were reported to exhibit only a weak carbonyl signal (Wang et al. 2010). Solid state ^{13}C NMR measurements of fluorescent carbon nanoparticles obtained from the combustion soot of candles displayed three types of carbon signals in the low field region of the spectrum (δ 110–180), assigned to external C=C, internal C=C, and C=O bonds (Liu et al.

2007). Furthermore, a recent ^{13}C NMR spectroscopic study of water-soluble carbon nanoparticles in D_2O suggested that the particles were of graphitic structure bearing peripheral carboxylic acid and carbonyl moieties, while the appearance of signals only in the δ 120–180 chemical shift range confirmed the presence of sp^2 hybridized aromatic carbon atoms and carbonyls (Tian et al. 2009).

In the present report, we turn our attention to the C-dot surface modifiers and apply 1D- and 2D-high-resolution ^1H and ^{13}C NMR spectroscopy in solution, taking advantage of the high solubility of the C-dots in either apolar or polar solvents, depending on modifier chemical structure. It was expected that the NMR studies would enable us to extract information about the sites where the modifier chain is bound on the C-dot and reveal the actual passivation mechanism. Due to line broadening effects, solution NMR spectroscopy is usually supposed to be of limited value in elucidating the structure and attachment mode of modifiers on the nanoparticle surface, and solid state HR-MAS techniques are thought to be more suitable tools (Du et al. 2009; Zhou et al. 2008). To our knowledge, this is the first detailed study in which the full structural assignment of the organic surface modifiers has been achieved by solution 1D and 2D NMR spectroscopy.

Experimental section

The synthesis of the three types of C-dots, Cwax, Cws, and Csalt (see Scheme 1) that were studied has already been described (Bourlinos et al. 2008a, b). Elemental analysis provided the tentative formula $(C_{18}H_{37}NH)(C_4O_{1.8})$, $(HOCH_2CH_2OCH_2CH_2NH)(C_{4.3}O_{2.1}H_{0.4})$ (Bourlinos et al. 2008a) and $(C_{3.3}O_3H_4)HN(CH_2)_{10}COONa$ (Bourlinos et al. 2008b) for Cwax, Cws, and Csalt, respectively.

NMR spectroscopy

Deuterated solvents ($CDCl_3$, D_2O, (99.96 atom % D) were obtained from Aldrich Chemical Co., Inc. 2–3 mg of C-dot were dissolved in 0.5 mL of deuterated solvent and transferred into a 5 mm NMR tube. ^1H and ^{13}C 1D NMR spectra were obtained on either a Bruker DPX-300 or a Bruker AMX-500 spectrometer using standard instrument software and pulse sequences (Braun and Kalinowski 1998), at a probe temperature of 299 K. For the ^{13}C NMR spectra, a line broadening of 1–20 Hz and drift correction were applied prior to Fourier transformation, depending on the natural linewidth of the ^{13}C signals, which varied with position on the modifier side chain. The linewidths reported in Fig. 5 are the natural linewidths of the carbon peaks, without any artificial line broadening. All NMR spectra were processed using TopSpin 3.0 software by Bruker. ^1H–^1H homonuclear gradient COSY 2D NMR spectra were obtained using 256 increments of 1 K data points, 128 scans and four dummy scans with a recycle delay of 1.5 s. ^1H–^{13}C heteronuclear gradient multiple quantum correlation (gHMQC) and multiple bond correlation (gHMBC) 2D NMR spectra were obtained using 128 increments of 1 K data points, 320 scans and four dummy scans with a recycle delay of 1.5 s. The gHMQC experiment was optimized for one bond ^1H–^{13}C couplings of 140 Hz by setting the evolution delay to 3 ms. The gHMBC experiment used an evolution delay of 60 ms optimized for long range ^1H–^{13}C J-couplings of $\sim$8 Hz (Braun and Kalinowski 1998). Before Fourier transformation all 2D data sets were zero-filled to a 1 $\times$ 1 K matrix, and a square-sinusoidal window function was used for processing.

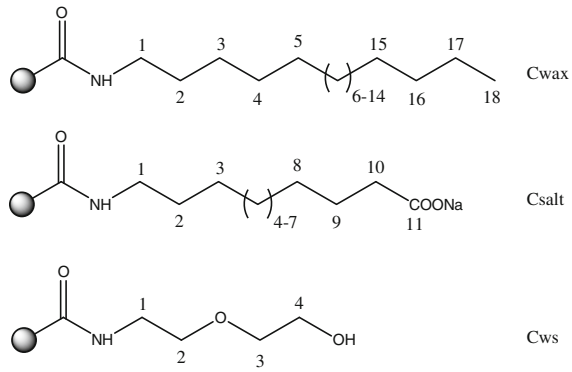

Scheme 1 Chemical structure of the C-dots: Cwax, Csalt, and Cws

Results and discussion

High-resolution solution 1D (^1H, ^{13}C) and 2D (gCOSY, gHMQC, gHMBC) NMR spectra were recorded for all three C-dots in either $CDCl_3$ or D_2O solutions depending on nanoparticle solubility, and used for their structural characterization. Figure 1 shows the ^1H and

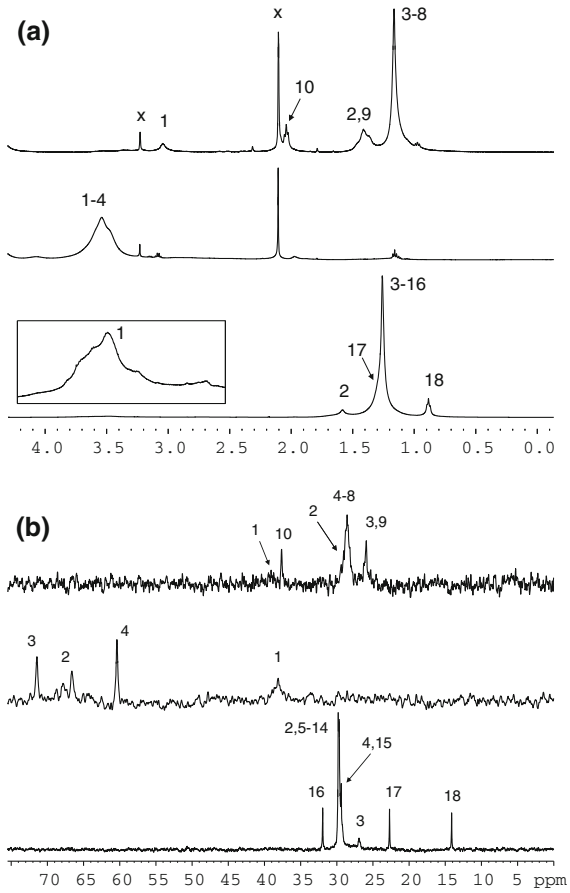

Fig. 1 ^{1}H NMR (**a**) and ^{13}C NMR (**b**) spectra of carbon dots Csalt (*up*), Cws (*middle*), and Cwax (*bottom*). The *inset* in (**a**) is a vertical expansion of the Cwax H_1 signal region. Peaks originating from solvent impurities are marked with *x*

^{13}C solution NMR spectra of the C-dots, while ^{1}H–^{13}C gCOSY, gHMQC, and gHMBC spectra of the samples are provided in Figs. 2, 3, and 4 respectively. Table 1 shows the chemical shifts (δ) of the main resonances in the ^{1}H and ^{13}C NMR spectra of all three C-dots, as obtained after the full analysis of their 1D and 2D NMR spectra. To our surprise, we found that all proton and carbon atoms of the three different modifiers could be directly observed in the 1D ^{1}H and ^{13}C NMR spectra, except carbons C-1 of Csalt and Cwax, which were only possible to identify in the respective ^{1}H–^{13}C gHMQC 2D NMR spectra (Fig. 3a, c), and amide protons. The suppression of amide proton signals in NMR spectra obtained in D_2O solution because of proton exchange with water molecules was not surprising, and $CDCl_3$ normally also contains traces of water. Another salient aspect of the analysis is that apart from the amide carbonyl group of the C-dots that lies on the nanoparticle surface, no signal arising from carbon atoms belonging to the nanoparticle nucleus was observed. This is in agreement with the only other liquid state NMR study of water-soluble C-dots reported (Tian et al. 2009), in which peripheral carboxylic acid and carbonyl moieties originating from the oxidative treatment of the nanoparticle surface were observed by ^{13}C NMR.

Csalt

Most of the protons of the Csalt modifier can be easily assigned by the analysis of the ^{1}H–^{1}H 2D gCOSY NMR spectrum of Fig. 2a. Of great interest is the low intensity signal at δ 3.1 corresponding to proton H_1, situated nearest to the amide bond, and the peak at δ 2.04 corresponding to the terminal methylene position H_{10}, adjacent to the carboxyl end group of the modifier. In Fig. 2a correlations between protons H_1–H_2–H_3 and H_{10}–H_9–H_8 are apparent, while protons H_4–H_7 appear as a broad feature at δ 1.26. The ^{13}C NMR spectrum of Csalt, presented in Fig. 1b (top) shows three rather broad peaks that cannot be assigned by direct chemical shift rules alone. The assignment of all the carbon atoms of Csalt was accomplished with the aid of the ^{1}H–^{13}C 2D NMR heteronuclear one bond (gHMQC, Fig. 3a) and multiple bond (gHMBC, Fig. 4) correlation spectra in D_2O solution. This also allowed the assignment of C_1, at δ 38.9, whose signal turned out to be too broad to be observed in the ^{13}C NMR spectrum of Fig. 1b. A cross peak between C_1 and H_1 is clearly visible in the gHMQC spectrum of Fig. 3a, while proton H_2 also displays a long range ($^{3}J_{CH}$) through bond correlation with C_1 in the gHMBC spectrum of Fig. 4. Several other long range C–H correlations are indicated in Fig. 4 that were used to successfully verify the correct assignment of the ^{1}H and ^{13}C 1D NMR spectra of Csalt.

Cws

As depicted in Fig. 1a, all four protons of Cws contribute to a broad spectral feature at δ 3.3–3.8, and cannot be resolved by ^{1}H NMR alone, since in this case the 2D gCOSY cannot provide any detailed information. However, the four different protons of Cws were separated and thus easily assigned with the help of the ^{1}H–^{13}C 2D heteronuclear correlation (gHMQC) spectrum, presented in Fig. 3b, thanks to

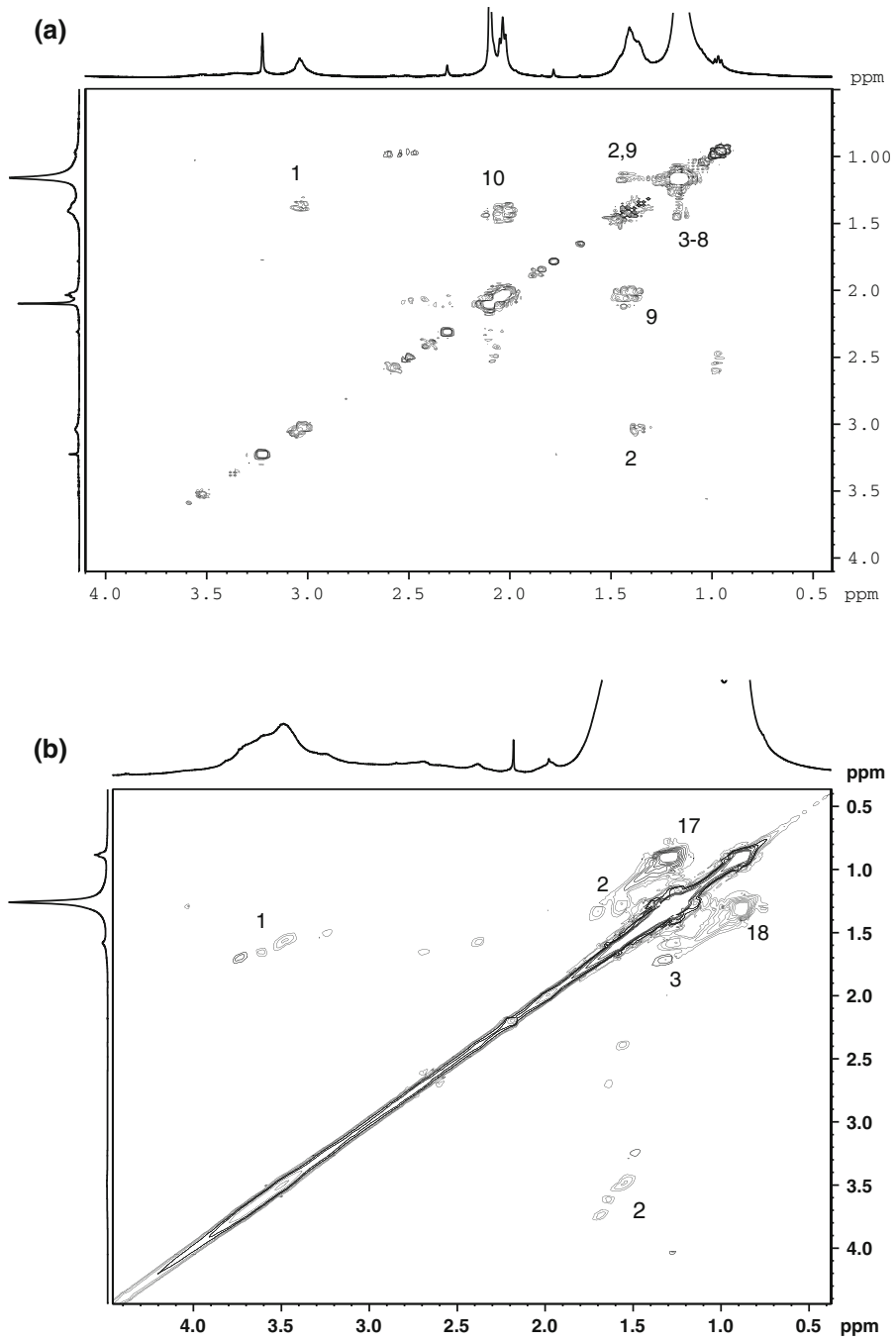

Fig. 2 ^{1}H–^{1}H gCOSY 2D NMR spectra of carbon dots, Csalt in D_2O solution (**a**) and Cwax in $CDCl_3$ solution (**b**). The gCOSY spectrum of Cws does not contain any useful information since all the protons fall on a single broad line (see Fig. 1)

the enhanced chemical shift resolution on the carbon frequency range. Carbon atoms C_1 and C_2 are situated closer to the nanoparticle surface and display broad and more dispersed signals in the carbon spectrum of Fig. 1b, indicative of significant structural heterogeneity on the attachment point of the modifiers to the nanoparticle surface, while C_3 and C_4 signals are significantly narrower.

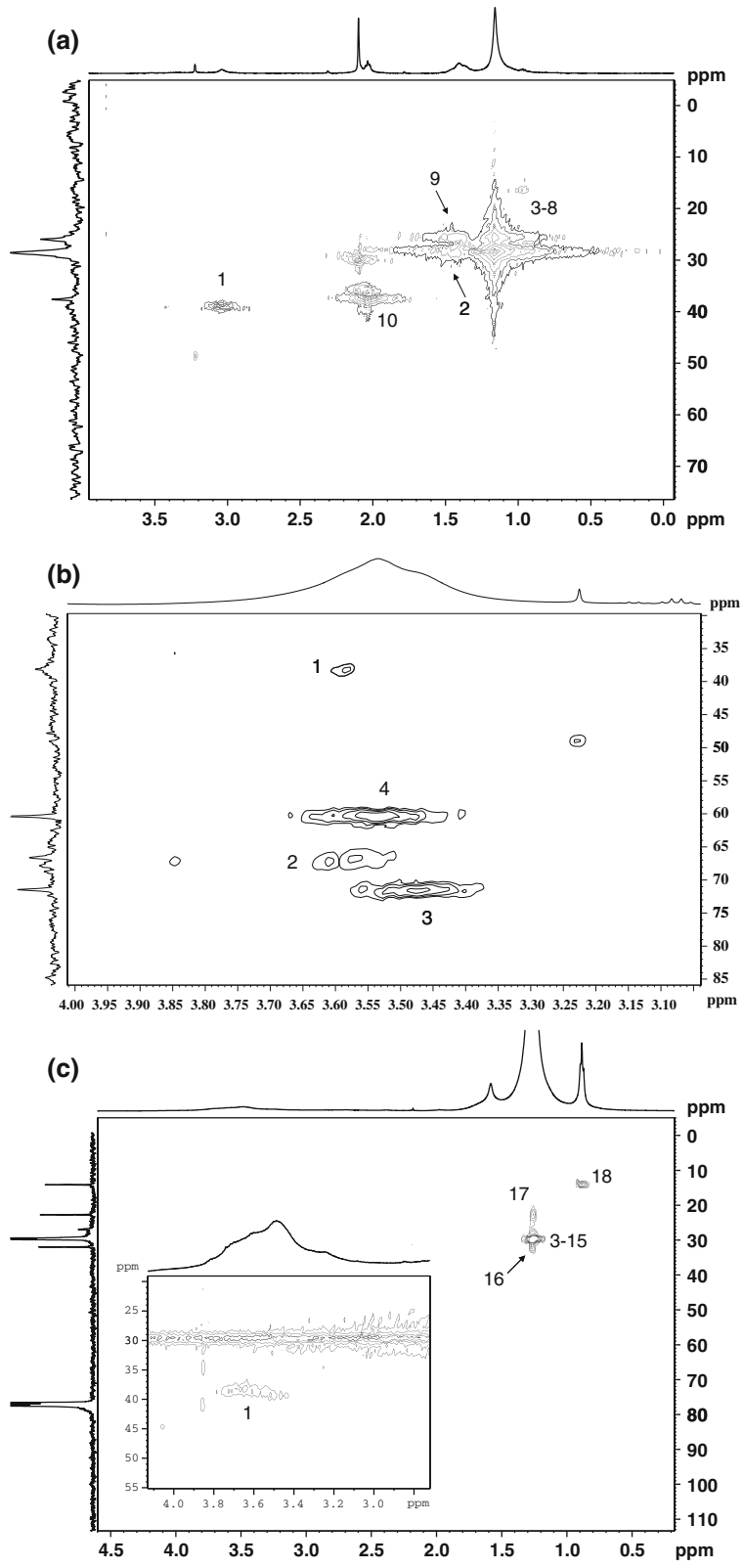

Fig. 3 ^{1}H–^{13}C gHMQC 2D NMR spectra of carbon dots Csalt in D_2O solution (**a**), Cws in D_2O solution (**b**), and Cwax in $CDCl_3$ solution (**c**)

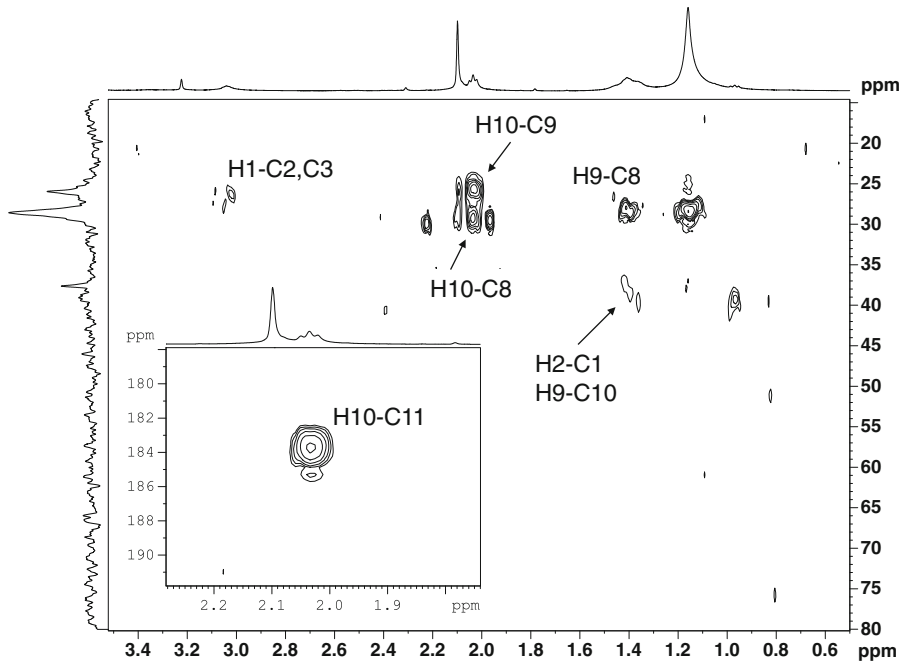

Fig. 4 ^{1}H–^{13}C gHMBC spectrum of carbon dot Csalt in D_2O solution. The *inset* shows the long range connectivity of H_{10} with the carbonyl carbon at $\delta \sim 184$

Table 1 ^{1}H and ^{13}C chemical shifts (δ) of the modifier resonances in the ^{1}H and ^{13}C NMR spectra of C-dots

Position	δ (ppm)					
	Csalt		Cws		Cwax	
	^{1}H	^{13}C	^{1}H	^{13}C	^{1}H	^{13}C
>C=O	–	176.5	–	177.3	–	177.6
1	3.1	38.9	3.59	38.4	3.5–3.7	38.7
2	1.46	28.6	3.56	67.9	1.58	29.8
3	1.16	26.3	3.46	71.6	1.26	27.0
4	1.15	28.4	3.53	60.4	1.26	29.4
5	1.15	28.4			1.26	29.7
6	1.15	28.4			1.26	29.75
7–8	1.15	28.4			1.26	29.75
9	1.41	25.8			1.26	29.75
10	2.04	37.7			1.26	29.75
11	–	183.7			1.26	29.75
12–14					1.26	29.75
15					1.26	29.4
16					1.26	31.9
17					1.32	22.7
18					0.88	14.1

Cwax

All the different protons of the C-wax side chain could be identified in the ^{1}H NMR spectrum of Fig. 1a. The broad feature at δ 3.5–3.7 (lower inset in Fig. 1a) corresponds to proton H_1 next to the amide bond, and importantly, very close to the linkage position of the modifier on the nanoparticle surface. This broad feature appears to comprise several peak components in the 2D gCOSY proton correlation spectrum of Cwax (Fig. 2c), implying a distribution of chemical environments for the modifier attachment point. The peak at δ 1.58 is assigned to H_2, as verified by its correlation with H_1 in the gCOSY spectrum, while the intense peak at δ 1.26 includes signals from methylene protons H_3–H_{16} in the middle of the aliphatic side chain. Although protons H_3–H_{16} cannot be resolved in the 1D spectrum, the higher spread of chemical shifts in the ^{13}C NMR spectrum allows the assignment of C_4–C_5 and C_{15}–C_{16}, which is further verified by the ^{1}H–^{13}C HMQC 2D NMR spectrum (see Fig. 3c). Positions 17 and 18 in the Cwax side chain are resolved in both the proton and carbon spectra, as reported in Table 1.

As expected, the proton and carbon peaks of C-dots in the 1D NMR spectra were significantly broadened, compared to those of the raw modifiers, which are well known (Tian et al. 2009). Figure 5 shows the ^{13}C NMR line widths (LW) at half height of all carbon atoms in the three C-dots as a function of position away from the amide linkage connecting the modifier to the nanoparticle surface. It is evident that line broadening is very large (LW > 100 Hz) for the position closest to the nucleus, C_1, where motional restrictions are very severe. Positions C_3–C_{10} still suffer from significant broadening (~20 Hz), while at the freely rotating end of the saturated chain modifier in Cwax, C_{15}–C_{18} LW are ~1 Hz, similar to those of carbon nuclei on free tumbling molecules in solution. The variation of ^{13}C line width with distance from the amide linkage reflects the intense mobility gradient enforced on the modifier chains by their attachment to the bulky C-dot core, as is well known in the case of linear aliphatic side chains attached to a macromolecular backbone (Spyros et al. 1995; Dais and Spyros 1995).

In summarizing the assignment of the NMR spectra of the three C-dots, a few important points are apparent:

(a) For all three types of C-dots, the chemical structure and attachment chemistry of the modifier chains was found to be in accordance with that proposed based on the organic materials used for C-dot synthesis, and there were no indications for chemical alteration of the modifiers during the passivation procedure.

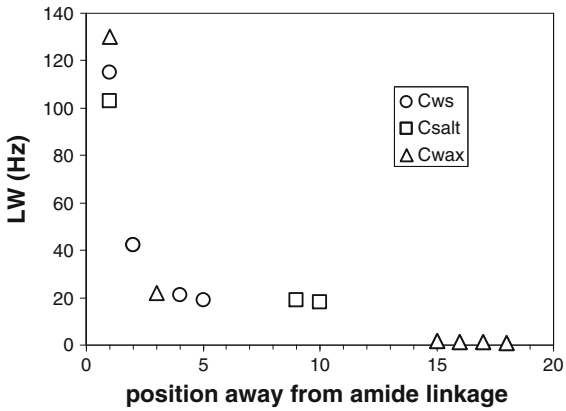

Fig. 5 ^{13}C NMR natural linewidths (Hz) of all modifier carbon atoms in the three C-dots as a function of position away from the amide linkage connection to the nanoparticle core

(b) The increased motional restriction closer to the nanoparticle surface attachment point may result in the practical disappearance of the NMR peaks of carbon nuclei situated very close to the binding site of the modifier chain by inducing large linewidth values, well over 100 Hz. However, it was demonstrated that 2D NMR heteronuclear correlation spectra can be used to recover missing information from the ^{13}C spectra. As depicted in the 2D gHMQC spectrum of Cwax and Csalt in Fig. 3, cross peaks caused due to the one bond *J*-coupling of C_1 with H_1 are prominent at δ 3.6/38.7 and δ 38.5/3.1 for Cwax and Csalt, respectively. These peaks can be used to infer the presence of C_1 in the modifier chain and thus verify the covalent attachment of the modifier to the nanoparticle nucleus.

(c) No NMR signals were observed for any of the C-dots studied in this report that could be attributed to carbons from the nanoparticle core. This result agrees with literature data on water-soluble nanoparticles obtained from natural gas soot (Tian et al. 2009) and is compatible with the proposed complete carbonization procedure of the nanoparticle core based on HR-TEM and XRD data (Bourlinos et al. 2008a, b). However, solid state NMR experiments are needed to fully confirm the core carbonization hypothesis and to further illuminate the chemical structure of the C-dot nucleus.

Conclusions

In the present report, we identified the precise chemical structure and attachment chemistry of the surface modifier chains in three different C-dots (Cwax, Cws, and Csalt). The full structural assignment of the C-dot organic modifier chains was achieved for the first time, by using exclusively solution 1D and 2D NMR spectroscopy. These results on the structure of C-dot modifiers will assist our understanding of the structure–optical activity relationship and may allow further tuning and control of the optical properties of C-dots. Current work focuses on the analysis of the structure of the carbon core of C-dots by solid state NMR spectroscopy. This is expected to provide evidence about the bonding among the carbon core atoms and further structural understanding of the

surface of C-dots, which so far remains rather elusive. Finally, it is hoped that since solution NMR spectroscopy proved to be highly effective in unambiguously identifying the structure of the surface modifiers in several soluble C-dots, its application as a structural characterization tool for nanoparticles and nanomaterials analysis will be further encouraged.

Acknowledgments This research was supported in part by the University of Crete (Project KA-3047) and the Operational Program Research and Development for Innovations-European Regional Development Fund (project CZ.1.05/2.1.00/03.0058) and Operational Program Education for Competitiveness (CZ.1.07/2.3.00/20.0017).

References

Baker SN, Baker GA (2010) Luminescent carbon nanodots: emergent nanolights. Angew Chem Int Ed 49:6726–6744

Bourlinos AB, Stassinopoulos A, Anglos D, Zboril R, Karakassides M, Giannelis EP (2008a) Surface functionalized carbogenic quantum dots. Small 4:455–458

Bourlinos AB, Stassinopoulos A, Anglos D, Zboril R, Georgakilas V, Giannelis EP (2008b) Photoluminescent carbogenic dots. Chem Mater 20:4539–4541

Braun S, Kalinowski HO (1998) 150 and more basic NMR experiments: a practical course, 2nd edn. Wiley, Weinheim

Cao L, Wang X, Meziani MJ, Lu FS, Wang HF, Luo PJG, Lin Y, Harruff BA, Veca LM, Murray D, Xie SY, Sun YP (2007) Carbon dots for multiphoton bioimaging. J Am Chem Soc 129:11318–11319

Dais P, Spyros A (1995) ^{13}C relaxation and local chain dynamics of synthetic polymers in solution and in the bulk. Progr NMR Spectrosc 27:555–633

Diaz D, Rivera M, Ni T, Rodriguez JC, Castillo-Blum SE, Nagesha DK, Robles J, Alvarez-Fregoso OJ, Kotov NA (1999) Conformation of ethylhexanoate stabilizer on the surface of CdS nanoparticles. J Phys Chem B 103: 9854–9858

Du F, Zhou H, Chen L, Zhang B, Yan B (2009) Structure elucidation of nanoparticle-bound organic molecules by ^{1}H NMR. Trends Anal Chem 28:88–95

Holland GP, Sharma R, Agola JO, Amin S, Solomon VC, Singh P, Buttry DA, Yarger JL (2007) NMR characterization of phosphonic acid capped SnO_2 nanoparticles. Chem Mater 19:2519–2526

Kitaygorodskiy A, Wang W, Xie SY, Lin Y, Shiral Fernando KA, Wang X, Qu L, Chen B, Sun YP (2005) NMR detection of single-walled carbon nanotubes in solution. J Am Chem Soc 127:7517–7520

Liu H, Ye T, Mao C (2007) Fluorescent carbon nanoparticles derived from candle soot. Angew Chem 119:6593–6595

Spyros A, Dais P, Marchessault RH (1995) Local chain motions of poly(*P*-hydroxyoctanoate) in the bulk. ^{13}C NMR relaxation study. J Polym Sci B 33:367–378

Suda Y, Ono T, Akazawa M, Sakai Y, Tsujino J, Homma N (2002) Preparation of carbon nanoparticles by plasma-assisted pulsed laser deposition method—size and binding energy dependence on ambient gas pressure and plasma condition. Thin Solid Films 415:15–20

Sun YP, Zhou B, Lin Y, Wang W, Shiral-Fernando KA, Pathak P, Meziani MJ, Harruff BA, Wang X, Wang H, Luo PG, Yang H, Kose ME, Chen B, Veca LM, Xie SY (2006) Quantum-sized carbon dots for bright and colorful photoluminescence. J Am Chem Soc 128:7756–7757

Tian L, Ghosh D, Chen W, Pradhan S, Chang X, Chen S (2009) Nanosized carbon particles from natural gas soot. Chem Mater 21:2803–2809

Tomaselli M, Yarger JL, Bruchez M, Havlin RH, deGraw D, Pines A, Alivisatos AP (1999) NMR study of InP quantum dots: surface structure and size effects. J Chem Phys 110:8861–8864

Wang X, Cao L, Yang ST, Lu F, Meziani MJ, Tian L, Sun KW, Bloodgood MA, Sun YP (2010) Bandgap-like strong fluorescence in functionalized carbon nanoparticles. Angew Chem 122:5438–5442

Willis AL, Turro NJ, O'Brien S (2005) Spectroscopic characterization of the surface of iron oxide nanocrystals. Chem Mater 17:5970–5975

Zhang B, Yan B (2010) Analytical strategies for characterizing the surface chemistry of nanoparticles. Anal Bioanal Chem 396:973–982

Zhou H, Du F, Li X, Zhang B, Li W, Yan B (2008) Characterization of organic molecules attached to gold nanoparticle surface using high resolution magic angle spinning ^{1}H NMR. J Phys Chem C 112:19360–19366